⌘ *Author's Choice*

THE JOURNAL OF BIOLOGICAL CHEMISTRY VOL. 284, NO. 48, pp. 33285–33295, November 27, 2009

Hydrophobic Core Mutations Associated with Cataract Development in Mice Destabilize Human γD-Crystallin*

Received for publication, June 10, 2009, and in revised form, September 14, 2009 Published, JBC Papers in Press, September 16, 2009, DOI 10.1074/jbc.M109.031344

Kate L. Moreau and Jonathan King[1]

From the Department of Biology, Massachusetts Institute of Technology, Cambridge, Massachusetts 02139

The human eye lens is composed of fiber cells packed with crystallins up to 450 mg/ml. Human γD-crystallin (HγD-Crys) is a monomeric, two-domain protein of the lens central nucleus. Both domains of this long lived protein have double Greek key β-sheet folds with well packed hydrophobic cores. Three mutations resulting in amino acid substitutions in the γ-crystallin buried cores (two in the N-terminal domain (N-td) and one in the C-terminal domain (C-td)) cause early onset cataract in mice, presumably an aggregated state of the mutant crystallins. It has not been possible to identify the aggregating precursor within lens tissues. To compare *in vivo* cataract-forming phenotypes with *in vitro* unfolding and aggregation of γ-crystallins, mouse mutant substitutions were introduced into HγD-Crys. The mutant proteins L5S, V75D, and I90F were expressed and purified from *Escherichia coli*. WT HγD-Crys unfolds *in vitro* through a three-state pathway, exhibiting an intermediate with the N-td unfolded and the C-td native-like. L5S and V75D in the N-td also displayed three-state unfolding transitions, with the first transition, unfolding of the N-td, shifted to significantly lower denaturant concentrations. I90F destabilized the C-td, shifting the overall unfolding transition to lower denaturant concentrations. During thermal denaturation, the mutant proteins exhibited lowered thermal stability compared with WT. Kinetic unfolding experiments showed that the N-tds of L5S and V75D unfolded faster than WT. I90F was globally destabilized and unfolded more rapidly. These results support models of cataract formation in which generation of partially unfolded species are precursors to the aggregated cataractous states responsible for light scattering.

The human lens is a tissue composed of onion-like layers of fiber cells. The lens core, or nucleus, is formed *in utero* and is composed of primary fiber cells. These cells are enucleated and devoid of all organelles, presumably to assist in maintaining transparency to visible light. During an individual's lifetime, lens epithelial cells, found in a single layer on the anterior portion of the lens, differentiate to become secondary fiber cells that surround the lens nucleus in layers, thus forming the lens outer cortex. Secondary fiber cells maintain their organelles and some level of protein synthesis and turnover.

The primary fiber cells of the lens have no protein synthesis or turnover. Thus, proteins translated *in utero* must maintain their native structure and remain soluble throughout the lifetime of the individual. The α-, β-, and γ-crystallins together account for 90% of lens proteins, present in concentrations of up to 450 mg/ml (1–3). α-Crystallin provides both structural and chaperone functions in the lens, whereas the β- and γ-crystallins appear to function solely as structural proteins (4–6). The continuous exposure of these proteins to environmental stresses, such as UV light and oxidizing agents, leads to the build-up of covalent damages (7–9). This can result in loss of native conformation and the generation of partially unfolded species that participate in aberrant protein-protein interactions. The resulting protein aggregation is likely to be a major pathway to cataract.

According to the World Health Organization, cataract is the leading cause of blindness worldwide. Age-related cataract affects at least 50% of people in the United States over age 80 (10). Comparison of age-related cataractons lenses with normal lenses identifies some significant differences between the two. The most obvious difference is the increase in accumulation of high molecular weight aggregates. Proteins isolated from cataractous lenses were found to be highly oxidized at cysteine and methionine residues (11, 12). Additional covalent modifications have been identified in aged lenses in general, including truncations (13–15), deamidation (7, 8, 16, 17), glycation of lysine residues (18), and oxidation of tryptophan (19). It is unclear whether these modifications, particularly the extensive oxidation, initiate the aggregation process or whether they are later effects, due to the trapping of partially unfolded species in the aggregate that are susceptible to damage. It is very plausible that accumulation of these various modifications destabilize lens crystallins, leading to their partial unfolding and exposure of hydrophobic core regions. Intermolecular interactions between these exposed regions could lead to aggregate formation, for example through a domain-swapping mechanism.

Since primary lens fiber cells lack nuclei and are terminally differentiated, they have not been propagated in tissue culture. In addition, studies of the initiation and growth of cataract within the intact lens have been very limited. As a result, it has not been possible to directly identify the state of crystallin precursors to cataract within lens fiber cells or the intact lens. We have attempted to circumvent this by examining the effects of mutations that cause cataracts in mice on the properties of human crystallin proteins *in vitro*.

Human γD-crystallin (HγD-Crys)[2] is a monomeric, two-domain protein whose structure has been determined at 1.25 Å

* This work was supported, in whole or in part, by National Institutes of Health Grants GM17980 and EY015834 (to J. K.).

⌘ *Author's Choice*—Final version full access.

[1] To whom correspondence should be addressed: 77 Massachusetts Ave., 68-330, Cambridge, MA 02139. Tel.: 617-253-4700; Fax: 617-252-1843; E-mail: jaking@mit.edu.

[2] The abbreviations used are: HγD-Crys, human γD-crystallin; MγS-Crys, murine γS-crystallin; N-td, N-terminal domain; C-td, C-terminal domain; GdnHCl, guanidinium hydrocholoride; DTT, dithiothreitol; WT, wild type.

(20), revealing two structurally homologous domains, each consisting of intercalated double Greek key motifs. HγD-Crys is one of the most abundant γ-crystallins found in the lens (21). It is primarily located in the central lens nucleus, the oldest region of the lens, and is therefore one of the longest lived proteins in that tissue as well as the entire human body. The two domains of HγD-Crys are connected by a short linker and interact through a set of hydrophobic interdomain contacts (22). Systematic studies of the unfolding and refolding of HγD-Crys have identified a partially folded intermediate with the N-terminal domain (N-td) unfolded and the C-terminal domain (C-td) folded (22, 23).

Rare mutations associated with juvenile onset cataracts have been identified in the human γ-crystallin genes. Those identified in HγD-Crys primarily affect charged surface residues, including R14C, R36S, R58H, and E107A (24–27); the non-surface mutation P23T has also been identified in families with inherited cataract (28–30). Truncations of human γ-crystallins also result in inherited, early onset cataract in some cases (28, 31). Previous studies with surface residue mutations have revealed that thiol-induced aggregation occurs in the case of R14C (32), whereas drastic decreases in solubility lead to crystallization of R36S and R58H mutant proteins (33). The P23T protein had reduced solubility (34, 35), although the thermodynamic stability was not affected, and structural studies at the atomic level revealed the altered conformation of an adjacent histidine residue (36). The human γC-crystallin T5P and R168W mutant proteins and human γS-crystallin G18V are three more amino acid substitutions affecting γ-crystallins that are associated with cataract formation (24, 37).

The crystallins are characterized by two classes of hydrophobic buried cores: the predominantly hydrophobic side chains within the β-sheets of the Greek Key motifs and the buried residues at the interface of the duplicated domains. Substitution of any of the six residues forming the hydrophobic domain interface of HγD-Crys resulted in a sharp destabilization of the native state and increased population of a partially folded intermediate with an unfolded N-td and folded C-td (22). Human families carrying mutations at sites in the tightly packed hydrophobic core of these proteins have not yet been reported. However, hydrophobic core mutations have been identified in murine crystallin genes (38–41). Murine γD-crystallin and HγD-Crys are closely related proteins of the same length with 83% sequence identity and 91% sequence similarity. Murine γS-crystallin (MγS-Crys) is more distantly related to HγD-Crys, because the vertebrate γS-crystallin lineage is believed to have diverged from other γ-crystallins earlier (42). Even considering this more distant relationship, MγS-Crys and HγD-Crys share 50% sequence identity and 70% sequence similarity.

Integrity of the hydrophobic core is generally vital for maintenance of a protein's tertiary structure. Studies on the N-terminal domain of the λ repressor showed that a wide range of amino acid substitutions in the protein core altered both structure and function (43). In particular, substitution of hydrophobic core residues with polar or charged residues resulted in large thermodynamic destabilizations *in vitro*. Dramatic decreases in biological activity were also observed, indicating that the structure was perturbed *in vivo* as well (43). In the case of SNase, the introduction of buried charges in the hydrophobic core was less disruptive due to local conformational changes that helped to stabilize the charges (44). A complete set of alanine substitutions in the P22 Arc repressor protein identified many destabilizing mutations. Five key residues, when substituted, resulted in polypeptide chains that did not appear to fold or adopt the native dimeric structure of the Arc repressor (45). Four of these five residues have hydrophobic side chains. In the 13-rung, parallel β-helix P22 tailspike adhesin, substitution with alanine of each of 140 residues in the elongated buried core resulted in folding defects for more than 100 of the mutant proteins (46).

The importance of the hydrophobic core has also been illustrated in the opposite sense, by stabilizing proteins through the introduction of hydrophobic residues. The concurrent substitution of three charged residues (Arg^{31}, Glu^{36}, and Arg^{40}) with the hydrophobic residues Met^{31}, Tyr^{36}, and Leu^{40} (MYL) in the Arc repressor resulted in a mutant protein that refolded with an apparent rate constant ~150-fold faster than the wild-type protein (47). Investigations on the hydrophobic core of T4 lysozyme found that compensatory "size switch" mutations destabilized the protein to a lesser extent than expected for additive effects (48). X-ray crystal structures of these mutants showed that the surrounding residues shifted to some extent to help accommodate the altered side chains. Hydrophobic protein cores appear to be quite sensitive to substitutions, and maintenance of ideal packing and geometries contribute greatly to protein stability.

The three amino acid substitutions, F9S in MγS-Crys (40, 49, 50) and V76D (38) and I90F (39) in murine γD-crystallin, are associated with congenital or early onset cataract in mice. Sinha *et al.* (40) previously identified the F9S substitution in MγS-Crys as causative for the murine *Opj* cataract phenotype (51, 52). Opacities, which increased in severity over time, were observed in the lenses of both *Opj/+* and *Opj/Opj* mice, although the phenotypes of the homozygotes were more severe. As a function of temperature *in vitro*, the F9S mutant displayed a loss of secondary structure and increased propensity for aggregation, both at lower temperatures than wild type (40). Wang *et al.* (53) found that lenses from mice homozygous for the V76D mutant allele contained intranuclear γ-crystallin protein aggregates and that the water-soluble γ-crystallin fraction of lens proteins was diminished. In transfection studies, the V76D mutant protein aggregated in both the nuclei and cytosol of cultured lens epithelial cells.

To further explore the effects of mutations to residues found in the hydrophobic core of HγD-Crys, we prepared a set of three HγD-Crys proteins carrying the murine amino acid replacements. All proteins were expressed in *Escherichia coli* and purified to study their overall conformation and thermodynamic and kinetic stabilities. Their significant destabilization highlights the importance of the tightly packed hydrophobic core of the γ-crystallins and sheds light on the possible mechanisms of congenital cataract formation associated with these mutations.

EXPERIMENTAL PROCEDURES

Mutagenesis, Expression, and Purification of Recombinant HγD-Crys—Constructs containing each of the three mutations, L5S, V75D, and I90F, were made by site-directed mutagenesis. Mutant primers (IDT-DNA) were used to amplify the HγD-Crys gene in the pQE.1 plasmid (Qiagen), which contains an N-terminal His_6 tag. Mutations were confirmed by sequencing of the entire gene (Massachusetts General Hospital).

Wild-type HγD-Crys and mutant proteins V75D and I90F were expressed as described previously (23). The mutant protein L5S was found in inclusion bodies in the insoluble portion of the cell lysate when expressed at physiological temperature. Overnight expression at 17 °C yielded a greater amount of natively folded protein. Cells were pelleted, resuspended in lysis buffer (50 mM NaP_i, 300 mM NaCl, 15 mM imidazole, pH 8.0), and stored at −80 °C.

Cells were lysed by ultrasonication, and insoluble cell debris was pelleted by centrifugation at 13,000 rpm for 45 min using an SS-34 rotor. Supernatants were filtered and applied to an Ni^{2+}-nitrilotriacetic acid column using an AKTA Purifier fast protein liquid chromatography system (GE Healthcare). Protein was eluted using a linear gradient of increasing imidazole. Fractions containing the protein of interest were pooled and dialyzed three times against 10 mM ammonium acetate, pH 7.0.

Circular Dichroism Spectroscopy—CD spectra of the wild-type and mutant proteins were obtained using an AVIV model 202 CD spectrometer (Lakewood, NJ). Protein samples were prepared at a concentration of 100 μg/ml in 10 mM NaP_i, pH 7.0. Spectra were collected from 260 to 195 nm in a 1-mm quartz cuvette held at 37 °C. Spectra were buffer-corrected, and mean residue ellipticity was calculated.

Fluorescence Emission Spectroscopy—Tryptophan fluorescence spectra of all proteins was measured using a Hitachi F-4500 fluorimeter. Samples contained protein at a concentration of 10 μg/ml in 100 mM NaP_i, 1 mM EDTA, 5 mM DTT, pH 7.0, and 5.5 M guanidinium hydrochloride (GdnHCl) for unfolded samples. An excitation wavelength of 295 nm was used to selectively excite tryptophan residues, and emission spectra were recorded from 310 to 400 nm and corrected for buffer signal.

Equilibrium Unfolding/Refolding—Equilibrium unfolding and refolding experiments were performed at 37 °C and pH 7.0 as described previously (54). The unfolding and refolding data were fit to a two-state (55) or three-state model (56) using the curve-fitting feature of the Kaleidagraph software package (Synergy Software). The increases in fluorescence of the refolding curves at low GdnHCl were due to light scattering resulting from protein aggregation of a partially folded intermediate into high molecular weight complexes. These points were not included in curve-fitting analysis. Transition midpoint, ΔG^0, and *m*-values were calculated for all transitions. Averages and S.D. values were calculated from three trials.

Thermal Denaturation—Thermal denaturation experiments were performed using an AVIV model 202 CD spectrometer. Temperature was monitored and raised with an internal Peltier thermoelectric controller. Samples were prepared as described above, except a 10-mm screw-top quartz cuvette was used to prevent evaporation of buffer at high temperatures. Changes in ellipticity at 218 nm were monitored every 1 °C from 25 to 90 °C. Sample temperature was allowed to equilibrate for 1 min before ellipticity was measured over a 3-s averaging time. Melting temperatures were determined by calculating the midpoints of transitions. Reported values are averages of three trials.

Unfolding Kinetics—All kinetic unfolding experiments were carried out at 18 °C. Experiments were performed by diluting wild-type and mutant proteins into 5.5 and 3.5 M GdnHCl, respectively, buffered with 100 mM NaP_i, 1 mM EDTA, 5 mM DTT, pH 7.0. Fluorescence emission at 350 nm was monitored over time using a Hitachi F-4500 fluorimeter with an excitation wavelength of 295 nm. Unfolding samples contained protein at a final concentration of 10 μg/ml. Kinetic unfolding data were fit with single or double exponentials, and residuals were calculated using the curve-fitting feature of Kaleidagraph. Best fits were chosen by agreement of calculated and observed parameters and a random distribution of residuals. Experiments were performed in triplicate for each protein, and parameters were averaged.

Refolding and Aggregation Turbidity Measurements—All protein samples at an initial concentration of 2 mg/ml were unfolded at 37 °C for at least 36 h in buffer (100 mM NaP_i, 1 mM EDTA, 5 mM DTT, pH 7.0) containing various concentrations of GdnHCl. Unfolded protein was placed in a quartz cuvette and diluted 20-fold with the appropriate buffer/GdnHCl solution to achieve a final protein concentration of 0.1 mg/ml and a final GdnHCl concentration of 0.17–0.18 M. The sample was immediately mixed after dilution by inverting the cuvette five times. It was then placed in a Cary 50 UV-visible spectrophotometer, and the solution turbidity was measured by the apparent absorbance at 350 nm for 20 min. All protein and buffer solutions were kept in a 37 °C water bath during the experiments, and the cuvette temperature was maintained at 37 °C using a single cell Peltier controller. All experiments for each protein were performed in triplicate. The refractive indices of the diluted solutions were measured to confirm that all samples contained the same final concentration of GdnHCl.

RESULTS

Protein Purification and Structural Characterization—To determine how these mutations, which have been linked to early onset cataract in mice, affect HγD-Crys, three human proteins were made: V75D, I90F, and L5S. (Numbering of residues is based on that of the wild-type HγD crystal structure, Protein Data Bank code 1HK0.) The residues Val^{75} and Ile^{90} are conserved and occur at identical positions in mouse and human γD-crystallins. The mutant alleles encoding V75D and I90F were constructed by site-specific mutagenesis of the human cDNA sequence cloned into the vector pQE1. The third mutation, encoding L5S, was constructed in a manner similar to that of the above mentioned mutations; however, this amino acid substitution was based on the cataract-associated F9S mutation in MγS-Crys (40). MγS-Crys has a four-residue N-terminal extension not found in mouse or human γD-crystallins. The homologous position in HγD-Crys to MγS-Crys F9S, based on protein sequence alignment, is Leu^5; thus, the nucleotides cor-

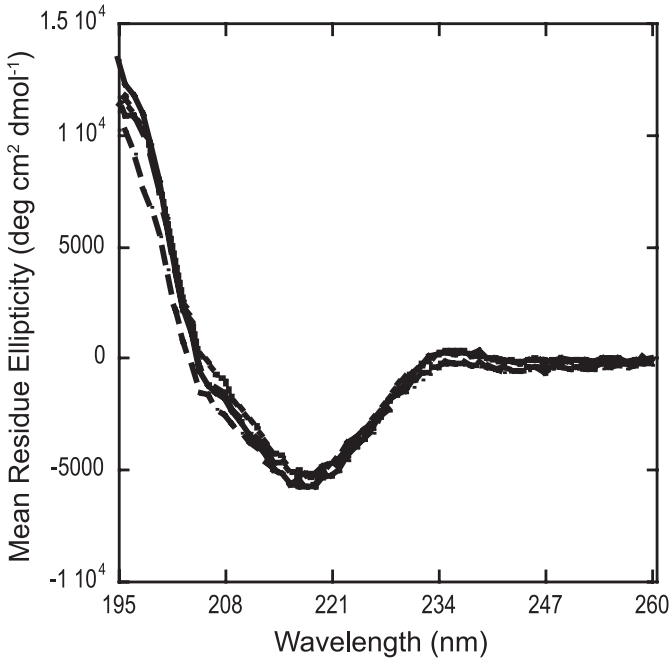

FIGURE 1. **Far-UV CD spectra of wild-type HγD-Crys (*solid black line*) and mutant proteins L5S (*short dashed line*), V75D (*long dashed line*), I90F (*dotted line*).** All proteins were present at 100 μg/ml in 10 mM NaP_i, pH 7.0. Spectra were collected at 37 °C.

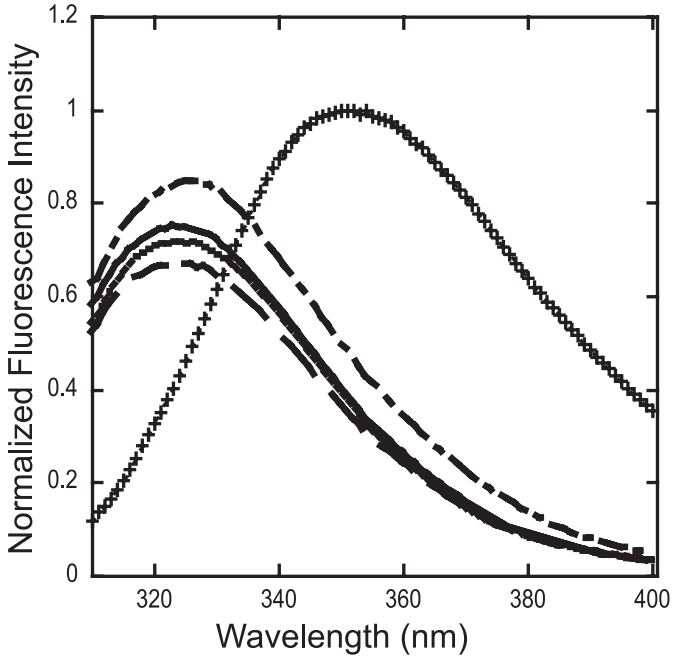

FIGURE 2. **Fluorescence spectra of native wild-type HγD-Crys (*solid black line*) and mutant proteins L5S (*dashed line*), V75D (*dotted dashed line*), and I90F (*dotted line*).** Normalized tryptophan fluorescence spectra of native wild-type protein and mutants is shown with fluorescence spectra of unfolded wild-type HγD-Crys (+) for comparison. Data were normalized to account for slight variations in concentrations. Spectra were collected at 37 °C. Protein solutions contained 100 mM NaP_i, 1 mM EDTA, 5 mM DTT, pH 7.0, with 5.5 M GdnHCl for the unfolded samples.

responding to this residue were changed to mimic this third mutation. Although this mutation is based on one described in MγS-Crys, this region in the first β-strand of the first Greek key motif appears to be important in other crystallins as well. The T5P substitution in γC-crystallin resulted in congenital cataract (24), and *in vitro* studies have found that the mutant protein had an altered conformation and lowered thermal stability (57).

All proteins were expressed in *E. coli* with N-terminal His_6 tags. When expressed at 37 °C, L5S was found in aggregates in the insoluble portion of the cell lysate. This indicates that this mutation affected the *in vivo* folding of the protein at physiological temperature. The L5S mutant protein was then expressed at 17 °C, and a greater portion was found in the soluble fraction of the cell lysate. These results are in line with observations by Sinha *et al.* (40), who observed thermal aggregation of the murine mutant protein F9S at temperatures as low as 46 °C. V75D and I90F proteins were expressed and soluble at 37 °C, indicating that these mutations did not affect the initial *in vivo* folding to the same extent as L5S. Both wild-type and mutant proteins were purified by Ni^{2+}-nitrilotriacetic acid affinity chromatography.

CD and fluorescence spectroscopy were used to compare the overall structures of the mutant proteins with that of wild-type HγD-Crys. These experiments distinguished any gross changes in secondary and tertiary structure among the mutant and wild-type proteins. The far-UV CD (Fig. 1) spectrum of wild-type HγD-Crys agreed with previous results (54). The spectrum displayed a minimum at 218 nm, indicative of high β-sheet content, and a small shoulder around 208 nm. The three mutant proteins displayed CD spectra with minima at 218 nm of similar intensity to wild type. L5S and I90F showed slight differences in the region around 208 nm, whereas V75D was indistinguishable from wild type in this region.

Tryptophan fluorescence was used to probe the overall tertiary structure of wild-type HγD-Crys and the three mutants. HγD-Crys has four buried tryptophan residues, arranged symmetrically between the two domains. It also contains 14 tyrosine residues, and an excitation wavelength of 295 nm was used to selectively excite the tryptophans. Trp fluorescence is strongly quenched in the native state of HγD-Crys compared with the unfolded state (58). Therefore, Trp fluorescence can be used as a sensitive indicator of tertiary structure for this protein. For the quenching to be maintained in mutant proteins, the tertiary structure of the native state cannot be greatly altered from that of WT. Otherwise, loss of quenching would be expected, due to the change in geometries of both the backbone and water molecules.

In agreement with previous experiments, native wild-type HγD-Crys had an emission maximum at about 326 nm (Fig. 2) (23). HγD-Crys unfolded in 5.5 M GdnHCl had a shifted emission maximum at 350 nm, which increased in intensity due to the loss of fluorescence quenching and energy transfer that is present in the native state (23, 58). Native L5S and I90F proteins both had fluorescence maxima at about 326 nm (Fig. 2). The peak fluorescence intensity of the native L5S protein was about 10% less than that of wild type, whereas that of I90F was very similar. Native V75D protein had a fluorescence maximum at 327 nm, and the peak fluorescence was about 13% greater that than of wild-type HγD-Crys (Fig. 2). These differences could be due to slight variations in solution conditions, or they may have been caused by slight structural perturbations around the Trp

TABLE 1
Equilibrium unfolding/refolding parameters for wild-type and mutant proteins at pH 7.0

Protein	Equilibrium transition 1			Equilibrium transition 2			Transitions 1 and 2 ($\Delta\Delta G^0_{N\rightarrow U}$)[d]
	C_m[a]	Apparent *m* value[b]	Apparent $\Delta G^0_{N\rightarrow I}$[c]	C_m[a]	Apparent *m* value[b]	Apparent $\Delta G^0_{I\rightarrow U}$[c]	
	M GdnHCl	*kcal/mol/M*	*kcal/mol*	*M GdnHCl*	*kcal/mol/M*	*kcal/mol*	*kcal/mol*
Wild type[e]	2.2 ± 0.1	3.6 ± 0.1	7.7 ± 0.2	2.8 ± 0.1	3.1 ± 0.4	8.9 ± 1.3	
L5S	0.7 ± 0.1	4.4 ± 0.2	3.1 ± 0.2	2.9 ± 0.1	3.1 ± 0.2	9.0 ± 0.4	4.6
V75D	0.8 ± 0.1	3.6 ± 1.1	2.9 ± 0.9	2.9 ± 0.1	3.0 ± 0.4	8.7 ± 1.1	5.0
I90F	1.7 ± 0.1	5.5 ± 1.2	9.4 ± 2.1				7.2

[a] Transition midpoints in units of M GdnHCl.
[b] Apparent *m* values in units of kcal/mol/M.
[c] Free energy of unfolding in the absence of GdnHCl in units of kcal/mol.
[d] $\Delta\Delta G_{N\rightarrow U} = (\Delta G^0_{N\rightarrow I(\text{wild type})} + \Delta G^0_{I\rightarrow U(\text{wild type})}) - (\Delta G^0_{N\rightarrow I(\text{mutant})} + \Delta G^0_{I\rightarrow U(\text{mutant})})$ in units of kcal/mol.
[e] Parameters of wild type are from Flaugh *et al.* (22).

side chains. Quenching of native state Trp fluorescence was observed for all mutants, further indicating that their structure was similar to that of WT.

Equilibrium Unfolding and Refolding of Wild-type and Mutant Human γD-Crystallins—Previously, equilibrium unfolding/refolding experiments were used to analyze the thermodynamic stability of wild-type HγD-Crys under physiological conditions (37 °C, pH 7.0) (22, 54, 59). These experiments utilized GdnHCl as the denaturing agent due to the fact that wild-type HγD-Crys does not fully unfold in up to 8 M urea (60). Tryptophan fluorescence was used to probe the conformation of proteins, and changes in fluorescence intensities at 360 and 320 nm were used for data analysis. Previous experiments found that the unfolding/refolding curves were best fit by a three-state model, which indicated the existence of a populated, partially folded intermediate with an unfolded N-td and a native-like C-td (22). The first transition, representing the unfolding of the N-td, had a midpoint of 2.2 M GdnHCl. The second transition, representing the unfolding of the C-td, had its midpoint at 2.8 M GdnHCl. The transition midpoints are at least 2 S.D. values apart, indicating that the two transitions are in fact separate (Table 1). Wild-type HγD-Crys chains aggregated upon refolding into buffer by dilution. Evidence for this aggregation was the distinct increase in scattering by the refolding samples at GdnHCl concentrations below 1 M.

Note that although the *y* axes in Fig. 3 describing equilibrium experiments are labeled as fluorescence intensity, the rise of the refolding curves at low GdnHCl concentrations is due to the right angle light scattering by the aggregated chains. atomic force microscopy images of these aggregated species can be seen in Ref. 60. Although the right angle scattering interferes with the fluorescence emission spectra of the aggregated species, a distinct red shift was still evident. This suggests that the chains in the aggregates are misfolded. Higher GdnHCl concentrations inhibit this off-pathway aggregation.

Thermodynamic stabilities of the three mutant proteins L5S, V75D, and I90F and WT HγD-Crys were analyzed by the same methods described above. Fluorescence data for all of the mutants were analyzed by changes in the fluorescence intensity at 360 nm. The data are shown as the ratio of fluorescence intensities at 360/320 nm for clarity. Parameters calculated for both sets of data agreed within the S.D. of the experiments.

The L5S substitution is in the first β-strand of the N-td of the protein. Similar to wild type, the data were fit by a three-state model, and the presence of a folding intermediate was indicated

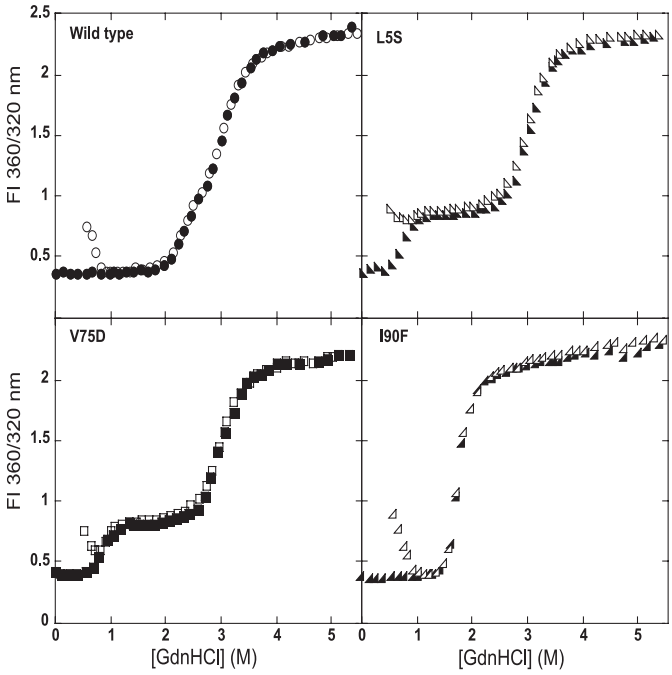

FIGURE 3. **Equilibrium unfolding (*solid symbols*) and refolding (*open symbols*) of wild-type HγD-Crys (●) and mutant proteins L5S (◣), V75D (■), and I90F (◢).** All proteins were present at 10 μg/ml in 100 mM NaP_i, 1 mM EDTA, 5 mM DTT, pH 7.0, and GdnHCl from 0 to 5.5 M. Measurements were collected at 37 °C. The ratio of fluorescence intensities at 360/320 nm is shown for visual clarity. Note that the increased fluorescence of the refolding curve at low GdnHCl concentrations represents light scattering due to aggregation and is not increased fluorescence intensity. All calculations were performed using single wavelength fluorescence emission data at 360 nm.

by a prominent plateau in the range of 1–2.3 M GdnHCl (Fig. 3 and Table 1). The first transition had a midpoint of ~0.72 M GdnHCl and an apparent $\Delta G^0_{N\rightarrow I}$ of 3.1 kcal/mol. The N-td is extremely destabilized compared with wild type, consistent with the location of the substitution. The midpoint of the second transition was ~2.9 M GdnHCl, and the apparent $\Delta G^0_{I\rightarrow U}$ was 9.0 kcal/mol. These values are very similar to those calculated for wild-type HγD-Crys. Thus, it appears that this substitution does not affect the stability of the C-td. Like the wild-type protein, L5S appeared to aggregate upon refolding into buffer as evidenced by the increase in fluorescence due to scattering from these refolding samples (Fig. 3). Unlike WT, this mutant protein was too destabilized to refold to a native-like conformation over the range of conditions present in these experiments.

The V75D substitution is located in the loop region between the fifth and sixth β-strands of the protein's N-td. The unfolding/refolding transitions of the V75D protein were quite similar to those of L5S and were also fit by a three-state model (Fig. 3 and Table 1). The first transition had a midpoint at 0.81 M GdnHCl and an apparent $\Delta G^0_{N\rightarrow I}$ of 2.9 kcal/mol. The second transition had a midpoint at 2.9 M GdnHCl and an apparent $\Delta G^0_{I\rightarrow U}$ of 9.0 kcal/mol. Like L5S, the V75D mutant had a dramatically destabilized N-td, consistent with the location of the amino acid substitution. The C-td was unaffected by this substitution and had a stability equal to that of wild-type HγD-Crys. The V75D protein also displayed aggregation behavior similar to that of L5S.

Unlike the previous two proteins, I90F was mutated at the start of the first β-strand in the C-td of the protein. Instead of the three-state transitions observed for wild-type, L5S, and V75D proteins, the unfolding/refolding data for I90F was fit by a two-state model (Fig. 3 and Table 1). This suggests that there is not a significantly populated intermediate in this transition. In agreement with this, the transition regions of the unfolding/refolding curves were clearly steeper than either transition region for the wild type, L5S, and V75D proteins. The midpoint of this single transition was at 1.7 M GdnHCl. This is lower than the midpoints of either transition for wild-type HγD-Crys. The apparent $\Delta G^0_{N\rightarrow U}$ for I90F was 9.4 kcal/mol. In a fashion similar to wild type, this mutant refolded to a native-like state at GdnHCl concentrations above 1 M but aggregated when diluted into buffer.

Thermal Unfolding of Wild-type and Mutant Human γD-Crystallins—Thermal unfolding employing a low ionic strength buffer was used as a second measure of stability of wild-type HγD-Crys and the three mutant crystallins. These experiments used a circular dichroism spectrophotometer to monitor changes in ellipticity at 218 nm from 25 to 90 °C. At high temperatures, all proteins aggregated, as shown by the clouding and opacification of all samples. With increasing temperature, the spectra exhibited reduced ellipticity of the 218 nm peak, representing loss of β-sheet structure and accumulation of both partially folded and aggregated species.

Confirming previous results (54), the thermal denaturation of wild-type HγD-Crys was fit by a two-state model without an obvious stable intermediate (Fig. 4). The melting temperature was 83.8 °C (Table 2). The thermal unfolding of the mutant protein V75D appeared overall to be two-state but with a gradual decrease in negative ellipticity from 40 to 50 °C. The melting temperature of this mutant was 71.7 °C (Fig. 4 and Table 2). In contrast, the thermal unfolding of the L5S and I90F proteins were best fit by three-state models. The first transition in the unfolding of L5S had a shallower slope with a midpoint at 57.4 °C. The second transition was much steeper, with a midpoint at 73.0 °C (Fig. 4 and Table 2). These results follow a similar pattern to those observed for the F9S MγS-Crys mutant compared with wild-type MγS-Crys (40). Thermal unfolding of the mutant I90F had a much flatter native base line and a small plateau in the transition region, corresponding to ~50% of the protein population existing in the native state. This indicates a populated intermediate on the unfolding pathway. The midpoint of the first transition was at 64.2 °C, and that of the second transition was 74.8 °C (Fig. 4 and Table 2).

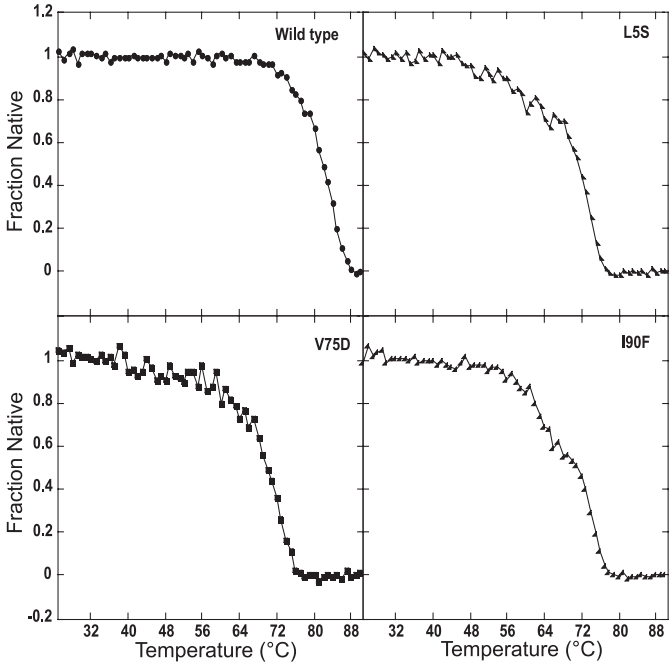

FIGURE 4. **Thermal unfolding of wild-type HγD-Crys and mutant proteins.** Unfolding was monitored by the change in ellipticity at 218 nm with increasing temperature. All proteins were present at 100 μg/ml in 10 mM NaP_i, pH 7.0. ●, wild-type HγD-Crys; ◣, L5S; ■, V75D; ◢, I90F.

TABLE 2
Thermal unfolding parameters of wild-type and mutant proteins at pH 7.0

Protein	Thermal unfolding transitions	
	T_{m1}[a]	T_{m2}[a]
	°C	
Wild type[b]	83.8 ± 1.3	
L5S	57.4 ± 2.8	73.0 ± 0.2
V75D	71.7 ± 0.2	
I90F	64.2 ± 0.5	74.8 ± 0.4

[a] Midpoints of melting transitions monitored by CD in units of °C.
[b] Thermal unfolding data of wild type are from Flaugh *et al.* (54).

Kinetic Unfolding of Wild-type and Mutant Human γD-Crystallins—To evaluate the effects of these mutations on the unfolding kinetics of HγD-Crys, we performed kinetic unfolding experiments by monitoring the increase in tryptophan fluorescence intensity at 350 nm over time when native protein was diluted into high concentrations of GdnHCl. All three mutant proteins unfolded very rapidly. To obtain unfolding rate constants, experimental conditions were altered to slow unfolding reactions. The three mutant proteins were rapidly diluted into 3.5 M GdnHCl, pH 7.0, at 18 °C. Wild-type HγD-Crys does not completely unfold under these conditions, so it was diluted into 5.5 M GdnHCl, pH 7.0, at 18 °C. These two sets of conditions enabled the measurement of unfolding rate constants and the calculation of unfolding half-times. Although rates may be not directly comparable, the use of 3.5 M GdnHCl emphasizes the destabilization induced by these mutations.

At 18 °C in 5.5 M GdnHCl, pH 7.0, the kinetic unfolding transitions of wild-type HγD-Crys (Fig. 5) were best fit by two exponentials. This suggests the presence of one unfolding intermediate,

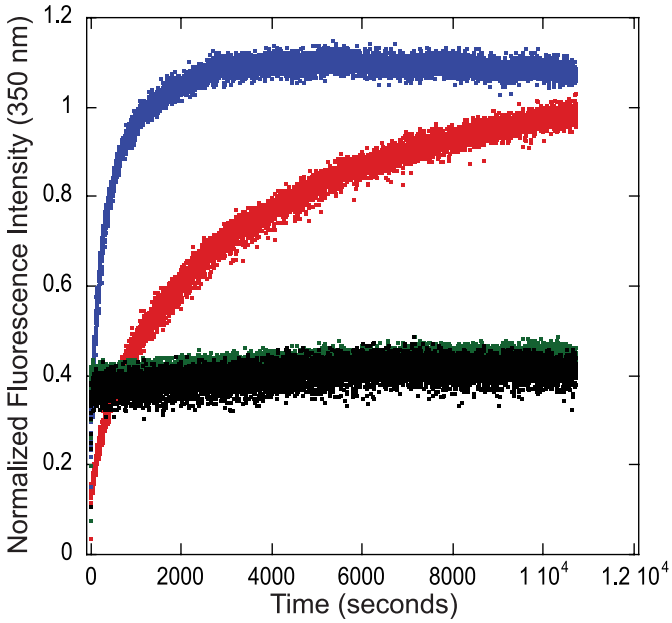

FIGURE 5. **Kinetic unfolding of wild-type HγD-Crys (*red*) and mutant proteins L5S (*green*), V75D (*black*), and I90F (*blue*).** All experiments were carried out at 18 °C at a final protein concentration of 10 μg/ml. Wild-type HγD-Crys was unfolded in 5.5 M GdnHCl, whereas all mutants were unfolded in 3.5 M GdnHCl to better measure kinetic parameters. All GdnHCl solutions were buffered with 100 mM NaP_i, 1 mM EDTA, 5 mM DTT, pH 7.0. The increase in fluorescence at 350 nm was used to monitor unfolding of the proteins. Fluorescence data were normalized for comparison. L5S and V75D are not completely unfolded at 3.5 M GdnHCl. See "Results" for details.

TABLE 3

Kinetic unfolding parameters of wild-type and mutant proteins at pH 7.0 and 18 °C

Protein	Kinetic unfolding transition 1		Kinetic unfolding transition 2	
	k_{u1}[a]	$t_{½}$[b]	k_{u1}[a]	$t_{½}$[b]
	s^{-1}	s	s^{-1}	s
Wild type	0.0017 ± 0.00017	403 ± 39	0.0002 ± 0.000029	3531 ± 502
L5S	0.32 ± 0.14	2.5 ± 1		
V75S	0.32 ± 0.065	2.0 ± 0.4		
I90F	0.0021 ± 0.00016	338 ± 28		

[a] Kinetic rate constants in units of s^{-1}.
[b] Half-times in units of s.

consistent with observations from equilibrium unfolding/refolding experiments. The unfolding transitions had $t_{½}$ values of 403 and 3531 s for the two phases, respectively (Table 3). These values were in agreement with previous results for HγD-Crys unfolding at 18 °C from Mills-Henry (61). Flaugh *et al.* (54) measured the kinetic unfolding transitions in 5.0 M GdnHCl, pH 7.0, at 37 °C. Their data were best fit by three exponentials with $t_{½}$ values of 0.79, 33, and 200 s for the three phases, respectively (54). It may be that this first transition was not discernible under the conditions employed here.

Kinetic unfolding rates of the mutant proteins were measured in a similar manner using the lower denaturant concentration of 3.5 M GdnHCl. The temperature and pH were maintained as for the wild-type protein. The kinetic unfolding transitions for the two mutant crystallins L5S and V75D were very similar (Fig. 5). They both exhibited an extremely rapid increase in fluorescence, which then reached a plateau over the course of 3 h. This plateau did not correspond to the fully unfolded protein but to ~40% of the chain existing in the unfolded state. The final fluorescence emission spectra of the unfolding samples were similar to the spectra for partially unfolded samples in equilibrium unfolding experiments (data not shown). This was consistent with the previous observation that neither wild-type HγD-Crys nor its isolated C-td unfolded completely in 3.5 M GdnHCl, pH 7.0, at 18 °C (61). Therefore, the rapid initial increases in fluorescence observed for both proteins most likely corresponded to the unfolding of the highly destabilized N-td, whereas the C-td remained folded. The observed unfolding transitions for L5S and V75D were fit by single exponentials, with $t_{½}$ values of 2.5 and 2.0 s, respectively (Table 3). In contrast, the mutant protein I90F unfolded completely under the same denaturant and temperature conditions utilized for the N-td mutants. The kinetic unfolding transition exhibited a rather rapid, steady rise in fluorescence (Fig. 5). This transition was best fit by a single exponential with a $t_{½}$ value of 338 s (Table 3). The final fluorescence emission spectra of the sample confirmed that the protein was completely unfolded.

Refolding and Aggregation of Partially Unfolded Wild-type and Mutant HγD-Crys—Both mutant proteins containing N-td amino acid substitutions, L5S and V75D, populated partially folded intermediates over a wide range of denaturant concentrations. The C-td mutant protein, I90F, did not appear to populate such an intermediate in the experiments described here. To determine whether the partially folded intermediates populated by the L5S and V75D proteins were aggregation-prone, proteins were partially unfolded in 0.2, 2, and 4 M GdnHCl at a concentration of 2 mg/ml under equilibrium conditions at 37 °C. The unfolding solutions at equilibrium were then diluted 20-fold to a final protein concentration of 100 μg/ml in ~0.2 M GdnHCl. These are conditions under which the mutant proteins were previously observed to aggregate when refolded from fully denatured state, represented here by the samples incubated in 4 M GdnHCl. Changes in the absorbance of the solution at 350 nm were monitored, with increasing absorbance indicating the formation of light scattering aggregates.

Both L5S and V75D proteins followed very similar aggregation patterns (Fig. 6). Aggregation upon dilution was only observed for samples that were fully denatured in 4 M GdnHCl. Partially unfolded samples that populated the observed folding intermediate did not form light scattering aggregates upon dilution. These results were similar to those obtained with the negative control samples. Wild-type HγD-Crys incubated under the same sets of conditions was only observed to aggregate when diluted out of 4 M GdnHCl, conditions under which the protein is fully unfolded. The N-td of the wild-type protein was only just beginning to unfold in 2 M GdnHCl, and no light scattering was seen when diluted from this condition.

The mutant protein I90F was treated somewhat differently because no obvious folding intermediate was observable in equilibrium unfolding/refolding experiments. 2 mg/ml protein samples were incubated at 37 °C in 0.2, 1.7, and 4.0 M GdnHCl until equilibrium was reached. 1.7 M GdnHCl was chosen as an intermediate concentration because this is the unfolding transition midpoint determined from GdnHCl-induced equilibrium unfolding/refolding experiments. Interestingly, during initial unfolding of the protein, the sample incubated in 1.7 M

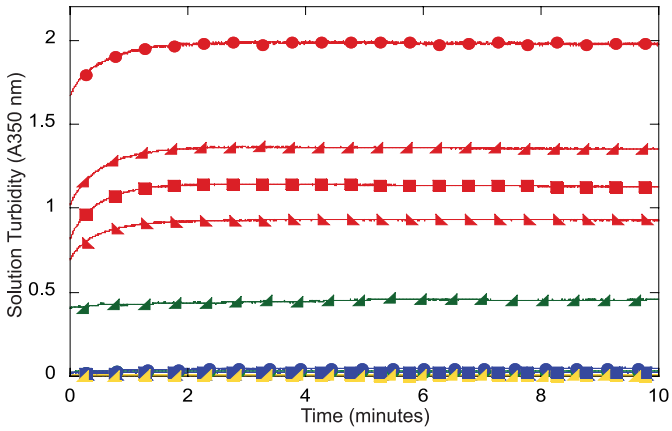

FIGURE 6. **Refolding aggregation of wild-type HγD-Crys (●) and mutant proteins L5S (◣), V75D (■), and I90F (◢).** All samples were incubated at 37 °C overnight at given concentrations of GdnHCl, indicated by the *color* of the *points/lines*: 4.0 M (*red*), 2.0 M (*blue*), 1.7 M (*green*), and 0.2 M (*yellow*). Protein samples were diluted with the appropriate buffer to a final denaturant concentration of ~0.2 M GdnHCl. Aggregation was monitored by measuring changes in absorbance at 350 nm over time.

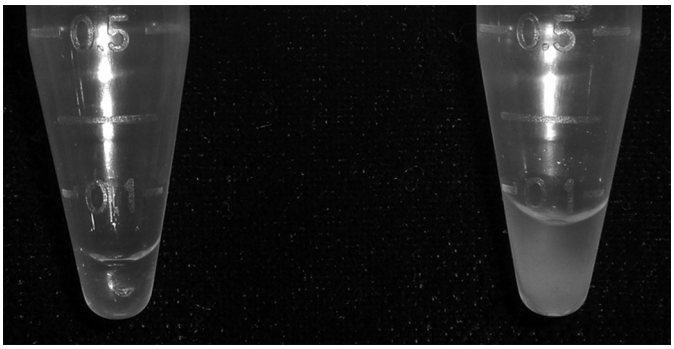

FIGURE 7. **Upon incubation of I90F (2 mg/ml) at 37 °C in 1.7 M GdnHCl, cloudy aggregates, visible by eye, formed that adhered to the sides of the microcentrifuge tube.** On the *right*, the aggregated I90F sample is shown. On the *left*, wild-type HγD-Crys incubated under the same conditions is shown. No aggregation was visible for the WT sample, and the solution turbidity was essentially zero over the course of the experiment.

GdnHCl began to aggregate (Fig. 7). The aggregate was visible by eye, and the protein solution appeared cloudy. This was the only sample among all proteins and denaturant concentrations for which this was observed. Because an obvious folding intermediate was not detectable by other methods, it is difficult to speculate on the mechanism of aggregation. When diluted 20-fold, the aggregates remained intact, and significant scatter was observed (Fig. 6). The level of scatter remained constant over the entire length of the experiment; there was no initial increase as observed for the fully unfolded samples that were diluted to induce aggregation. As expected, the fully unfolded I90F protein aggregated upon dilution with buffer in a manner similar to all other fully unfolded (4.0 M GdnHCl) samples (Fig. 6).

DISCUSSION

As a result of the physical integrity of the lens, it has been difficult to study cataract formation in the native environment. Thus, direct evidence linking the aggregation reactions documented *in vitro* with cataract formation *in situ* has been lacking. We have attempted to bridge this gap by characterizing the effects of mouse crystallin cataract-causing mutations on human lens crystallins.

For a number of protein aggregation diseases, partially unfolded chains are thought to be the precursors in the aggregation reactions (62). The γ-crystallins appear to have an extremely rigid three-dimensional structure with tight side chain packing (63). The three cataract-associated mutations were chosen to investigate the effects of mutation on the tightly packed hydrophobic core of HγD-Crys. All three mutations investigated dramatically destabilized HγD-Crys in equilibrium unfolding/refolding experiments. Overall ΔG^{o} values were decreased by 4.6 and 5.0 kcal/mol for L5S and V75D mutant crystallins, respectively. For I90F, the ΔG^{o} value decreased by 7.2 kcal/mol in comparison with wild-type HγD-Crys. The site of the substitution was directly related to the domain destabilization. For the two N-td mutants, L5S and V75D, only the stability of the N-td was affected, in that its unfolding transition midpoint was lowered. The C-td unfolding transition midpoint was not affected in either case. For the I90F substitution, which is found in the C-td, a steep two-state transition was observed with no discernible intermediates. This indicates that both domains are destabilized and the entire protein is globally unfolding without significantly populated intermediates. Previous work showed that HγD-Crys folds through a three-state pathway with the C-td folding first, followed by the N-td (23). Destabilization of the C-td may result in global protein destabilization because the domain interface, which is known to play a role in HγD-Crys stability (22), may not be in its native conformation.

Wild-type HγD-Crys is resistant to thermal denaturation; its melting temperature is ~83 °C. The three amino acid replacements lowered the melting temperatures, and the melting curves for all mutant proteins indicated a population of partially unfolded intermediates. However, because these data are based on CD measurements of overall secondary structure, decreases in melting temperature and appearance of possible intermediates cannot be attributed to specific regions of the protein's three-dimensional structure. This is in contrast to the tryptophan fluorescence unfolding data, which reports on the regions of the protein surrounding the buried tryptophans.

In kinetic experiments, all three mutant proteins unfolded faster than wild-type HγD-Crys. Previously, it was shown that wild-type HγD-Crys requires 1 h in 5.5 M GdnHCl at 37 °C to unfold completely (54). Under these conditions, all three mutant proteins unfolded within the dead time of the experiment (~1 s). Experimental conditions were altered to 3.5 M GdnHCl and 18 °C to slow unfolding and enable observation of the unfolding transition(s) by changes in tryptophan fluorescence. Under these altered conditions, the wild-type protein will not fully unfold. This fact alone attests to the dramatic destabilizing effects of these substitutions on HγD-Crys.

Similar to the results of the equilibrium unfolding/refolding experiments, the location of the mutation corresponded with the observed kinetic destabilization. For both N-td substitutions L5S and V75D, the single kinetic transition observed for each mutant protein most likely corresponded to the unfolding of the N-td. Our results further support the observation that mutations in the N-td, even at different locations within the

domain, appear to solely affect that domain's stability. Mills-Henry and colleagues (61) found that the extrapolated *in vitro* unfolding half-time of wild-type HγD-Crys in the absence of denaturant was ~19 years. This number is probably greatly reduced for all of the mutants investigated here. A hysteresis was observed in previous equilibrium unfolding/refolding experiments, particularly for the unfolding of the N-td of full-length HγD-Crys (60). It was concluded that the domain interface contributed substantially to the kinetic stability of the protein. The large destabilization of the N-td for both the L5S and V75D proteins disrupts the interactions at the domain interface, and this may contribute to an overall destabilization of the protein. Further kinetic analysis could address this issue.

In contrast, the C-td mutant I90F completely unfolded through a single observable kinetic transition, most likely the simultaneous unfolding of both domains. In agreement with equilibrium data, the disruption of the C-td by I90F resulted in destabilization of the entire protein. The N-td cannot remain folded if the C-td is unfolded in the full-length protein. However, Mills *et al.* showed that the isolated N-terminal domains of HγD-Crys and human γS-crystallin fold into distinct structures that exhibit the fluorescence quenching characteristic of the γ-crystallins and tryptophan fluorescence spectra similar to the full-length proteins (64). Therefore, the N-td of HγD-Crys in isolation is capable of folding. Nonetheless, in the context of the full-length protein, the C-td must be fully folded with its domain interface contacts available for proper folding of the N-td. The simplest model to explain these data is that the interface formed by the C-td is used as a template for folding of the N-td.

The effects of these mutations on the kinetic and thermodynamic stabilities of HγD-Crys are in line with studies of other proteins, as described in the Introduction (22, 43–46). The introduction of a charged side chain into the protein core with the V75D substitution was extremely destabilizing, and a slight increase in native state fluorescence measurements indicates possible local perturbations in structure, particularly around the Trp residues in the N-td. The L5S substitution also introduces a polar residue into the core and most likely creates a cavity due to the introduction of a much smaller side chain. This could be very destabilizing due to the loss of favorable van der Waals interactions. Filling of cavities in the hydrophobic protein core has been shown to be stabilizing in some cases (65). The experimental results presented here for L5S support and complement the work previously discussed (40). The destabilization resulting from the substitution of phenylalanine for isoleucine at position 90 is probably due to the introduction of a large bulky aromatic residue. Although this substitution retains the hydrophobic nature of the side chain, the increase in volume may introduce strain or disrupt other favorable interactions that are stabilizing the protein structure.

In contrast to the surface substitutions linked to congenital and early onset cataract, the effect of these mutations is destabilization of the native state of HγD-Crys. The mutant proteins also unfolded significantly faster under less denaturing conditions than wild type. This implies that their unfolding half-life in non-denaturing conditions may also be significantly shortened. Lens proteins are synthesized early in life, and there is no protein turnover after birth in the central, innermost regions of the lens. The accumulation in the lens of partially or fully unfolded crystallins at extremely high concentrations may saturate the finite α-crystallin population, which is the only mechanism present in the lens nucleus for binding and sequestering partially unfolded or misfolded proteins.

Aggregation of HγD-Crys Requires Partial Unfolding of C-terminal Domain—For proteins with duplicated domains, the simplest pathway to polymerization would be a domain swap mechanism (66). This type of interaction is naturally occurring for βB2-crystallin (67), whose crystal structure was found to be a dimer. Aggregation by a domain swap mechanism has not yet been observed for the crystallins but has been documented for cystatin C (68). Models of aggregation by domain swapping have been hypothesized for the human prion protein (69) and β2-microglobulin (70) based on a wide range of structural analysis.

Contrary to the simplest form of the domain swap hypothesis, the partially folded intermediates investigated here did not form aggregates under these experimental conditions. For all proteins, both wild-type and mutant, it seems that at least partial unfolding of the C-td was necessary for aggregation to occur. This hints at a possible β-strand insertion mechanism of aggregation, where at least one β-strand from one molecule of HγD-Crys is inserted into the domain of a second molecule. This may be somewhat similar to the β-sheet expansion modeled for serpin polymerization (71). (Yamasaki *et al.* (71) refer to this mechanism of polymerization as domain swapping. For our discussion of the crystallins, we have used "domain swapping" to refer to the exchange of the entire N-terminal or C-terminal domains.) The aggregation of the mutant protein I90F even at intermediate GdnHCl concentrations emphasizes the strength of the intermolecular interactions occurring in these polymeric species.

The cloudiness and precipitation observed for this sample was most likely not a result of phase separation. Pande *et al.* (35) showed that phase separation occurs for the inherited cataract mutant P23T HγD-Crys. P23T separated into two phases, one consisting of monomers and the other consisting of clusters of protein that precipitated out of solution. It was demonstrated that this phase change occurred without changes in protein structure and furthermore shown that this mutant does not have altered thermal stability compared with WT. In contrast, I90F had decreased stability, and the observed aggregation only occurred when the protein was subjected to partially denaturing conditions. The protein remained soluble under native conditions.

Both bovine and human γ-crystallins have been shown to form amyloid fibrils under partially denaturing, acidic conditions (72, 73). Fibrillar structures have been observed by thin section transmission electron microscopy in both the *Opj/Opj* mouse lens (40) and the OXYS rat lens (74), from a strain that generates excessive reactive oxygen species. Although the *Opj* and OXYS phenotypes lead to cataract, they may affect lens development as well as lens opacity and function. Due to the high β-sheet content of the γ-crystallins, there may be underlying similarities between their mechanisms of amyloid formation and the aggregation pathways observed in both our and the

aforementioned studies. The molecular basis of γ-crystallin aggregation is an area that warrants further investigation. The correlation between the cataract phenotype of the single amino acid substitutions in the mouse crystallins and the *in vitro* thermodynamic and kinetic destabilization of the purified human mutant proteins supports models of cataract formation following from protein conformational change and aggregation.

Acknowledgments—We thank Dr. Ishara Mills-Henry, Dr. Jiejin Chen, Ligia Acosta Sampson, and Dr. Kelly Knee for many helpful discussions. The Biophysical Instrumentation Facility for the Study of Complex Macromolecular Systems (supported by National Science Foundation Grant 0070319 and National Institutes of Health Grant GM68762) is gratefully acknowledged.

REFERENCES

1. Fagerholm, P., Philipson, B., and Carlström, D. (1981) *Curr. Eye Res.* **1,** 629–633
2. Slingsby, C., and Clout, N. J. (1999) *Eye* **13,** 395–402
3. Siezen, R. J., Wu, E., Kaplan, E. D., Thomson, J. A., and Benedek, G. B. (1988) *J. Mol. Biol.* **199,** 475–490
4. Horwitz, J. (1992) *Proc. Natl. Acad. Sci. U.S.A.* **89,** 10449–10453
5. Boyle, D., and Takemoto, L. (1994) *Exp. Eye Res.* **58,** 9–15
6. Jaenicke, R., and Slingsby, C. (2001) *Crit. Rev. Biochem. Mol. Biol.* **36,** 435–499
7. Hanson, S. R., Hasan, A., Smith, D. L., and Smith, J. B. (2000) *Exp Eye Res* **71,** 195–207
8. Hanson, S. R., Smith, D. L., and Smith, J. B. (1998) *Exp. Eye Res.* **67,** 301–312
9. Hoenders, H. J., and Bloemendal, H. (1983) *J. Gerontol.* **38,** 278–286
10. Prevent Blindness America and NEI, National Institutes of Health (2008) *Vision Problems in the U.S.: Prevalence of Adult Vision Impairment and Age-Related Eye Disease in America*, 4th Ed., pp. 22–25, Prevent Blindness America and NEI, National Institutes of Health
11. Truscott, R. J., and Augusteyn, R. C. (1977) *Biochim. Biophys. Acta* **492,** 43–52
12. Truscott, R. J., and Augusteyn, R. C. (1977) *Exp. Eye Res.* **25,** 139–148
13. Ajaz, M. S., Ma, Z., Smith, D. L., and Smith, J. B. (1997) *J. Biol. Chem.* **272,** 11250–11255
14. Takemoto, L., and Emmons, T. (1991) *Exp. Eye Res.* **53,** 811–813
15. Zhang, Z., Smith, D. L., and Smith, J. B. (2003) *Exp. Eye Res.* **77,** 259–272
16. Lampi, K. J., Ma, Z., Hanson, S. R., Azuma, M., Shih, M., Shearer, T. R., Smith, D. L., Smith, J. B., and David, L. L. (1998) *Exp. Eye Res.* **67,** 31–43
17. Ma, Z., Hanson, S. R., Lampi, K. J., David, L. L., Smith, D. L., and Smith, J. B. (1998) *Exp. Eye Res.* **67,** 21–30
18. Chiou, S. H., Chylack, L. T., Jr., Tung, W. H., and Bunn, H. F. (1981) *J. Biol. Chem.* **256,** 5176–5180
19. Hains, P. G., and Truscott, R. J. (2007) *J. Proteome Res.* **6,** 3935–3943
20. Basak, A., Bateman, O., Slingsby, C., Pande, A., Asherie, N., Ogun, O., Benedek, G. B., and Pande, J. (2003) *J. Mol. Biol.* **328,** 1137–1147
21. Lampi, K. J., Ma, Z., Shih, M., Shearer, T. R., Smith, J. B., Smith, D. L., and David, L. L. (1997) *J. Biol. Chem.* **272,** 2268–2275
22. Flaugh, S. L., Kosinski-Collins, M. S., and King, J. (2005) *Protein Sci.* **14,** 569–581
23. Kosinski-Collins, M. S., Flaugh, S. L., and King, J. (2004) *Protein Sci.* **13,** 2223–2235
24. Héon, E., Priston, M., Schorderet, D. F., Billingsley, G. D., Girard, P. O., Lubsen, N., and Munier, F. L. (1999) *Am. J. Hum. Genet.* **65,** 1261–1267
25. Kmoch, S., Brynda, J., Asfaw, B., Bezouska, K., Novák, P., Rezácová, P., Ondrová, L., Filipec, M., Sedlácek, J., and Elleder, M. (2000) *Hum. Mol. Genet.* **9,** 1779–1786
26. Stephan, D. A., Gillanders, E., Vanderveen, D., Freas-Lutz, D., Wistow, G., Baxevanis, A. D., Robbins, C. M., VanAuken, A., Quesenberry, M. I., Bailey-Wilson, J., Juo, S. H., Trent, J. M., Smith, L., and Brownstein, M. J. (1999) *Proc. Natl. Acad. Sci. U.S.A.* **96,** 1008–1012
27. Messina-Baas, O. M., Gonzalez-Huerta, L. M., and Cuevas-Covarrubias, S. A. (2006) *Mol. Vis.* **12,** 995–1000
28. Santhiya, S. T., Shyam Manohar, M., Rawlley, D., Vijayalakshmi, P., Namperumalsamy, P., Gopinath, P. M., Löster, J., and Graw, J. (2002) *J. Med. Genet.* **39,** 352–358
29. Nandrot, E., Slingsby, C., Basak, A., Cherif-Chefchaouni, M., Benazzouz, B., Hajaji, Y., Boutayeb, S., Gribouval, O., Arbogast, L., Berraho, A., Abitbol, M., and Hilal, L. (2003) *J. Med. Genet.* **40,** 262–267
30. Burdon, K. P., Wirth, M. G., Mackey, D. A., Russell-Eggitt, I. M., Craig, J. E., Elder, J. E., Dickinson, J. L., and Sale, M. M. (2004) *Br. J. Ophthalmol.* **88,** 79–83
31. Hansen, L., Yao, W., Eiberg, H., Kjaer, K. W., Baggesen, K., Hejtmancik, J. F., and Rosenberg, T. (2007) *Invest. Ophthalmol. Vis. Sci.* **48,** 3937–3944
32. Pande, A., Pande, J., Asherie, N., Lomakin, A., Ogun, O., King, J. A., Lubsen, N. H., Walton, D., and Benedek, G. B. (2000) *Proc. Natl. Acad. Sci. U.S.A.* **97,** 1993–1998
33. Pande, A., Pande, J., Asherie, N., Lomakin, A., Ogun, O., King, J., and Benedek, G. B. (2001) *Proc. Natl. Acad. Sci. U.S.A.* **98,** 6116–6120
34. Evans, P., Wyatt, K., Wistow, G. J., Bateman, O. A., Wallace, B. A., and Slingsby, C. (2004) *J. Mol. Biol.* **343,** 435–444
35. Pande, A., Annunziata, O., Asherie, N., Ogun, O., Benedek, G. B., and Pande, J. (2005) *Biochemistry* **44,** 2491–2500
36. Jung, J., Byeon, I. J., Wang, Y., King, J., and Gronenborn, A. M. (2009) *Biochemistry*, **48**, 2597–2609
37. Sun, H., Ma, Z., Li, Y., Liu, B., Li, Z., Ding, X., Gao, Y., Ma, W., Tang, X., Li, X., and Shen, Y. (2005) *J. Med. Genet.* **42,** 706–710
38. Graw, J., Löster, J., Soewarto, D., Fuchs, H., Reis, A., Wolf, E., Balling, R., and Hrabé de Angelis, M. (2002) *Mamm. Genome* **13,** 452–455
39. Graw, J., Neuhäuser-Klaus, A., Klopp, N., Selby, P. B., Löster, J., and Favor, J. (2004) *Invest. Ophthalmol. Vis. Sci.* **45,** 1202–1213
40. Sinha, D., Wyatt, M. K., Sarra, R., Jaworski, C., Slingsby, C., Thaung, C., Pannell, L., Robison, W. G., Favor, J., Lyon, M., and Wistow, G. (2001) *J. Biol. Chem.* **276,** 9308–9315
41. Graw, J., Klopp, N., Neuhäuser-Klaus, A., Favor, J., and Löster, J. (2002) *Invest. Ophthalmol. Vis. Sci.* **43,** 2998–3002
42. Wistow, G., Wyatt, K., David, L., Gao, C., Bateman, O., Bernstein, S., Tomarev, S., Segovia, L., Slingsby, C., and Vihtelic, T. (2005) *FEBS J.* **272,** 2276–2291
43. Lim, W. A., Farruggio, D. C., and Sauer, R. T. (1992) *Biochemistry* **31,** 4324–4333
44. Denisov, V. P., Schlessman, J. L., García-Moreno, E. B., and Halle, B. (2004) *Biophys. J.* **87,** 3982–3994
45. Milla, M. E., Brown, B. M., and Sauer, R. T. (1994) *Nat. Struct. Biol.* **1,** 518–523
46. Simkovsky, R., and King, J. (2006) *Proc. Natl. Acad. Sci. U.S.A.* **103,** 3575–3580
47. Waldburger, C. D., Jonsson, T., and Sauer, R. T. (1996) *Proc. Natl. Acad. Sci. U.S.A.* **93,** 2629–2634
48. Baldwin, E., Xu, J., Hajiseyedjavadi, O., Baase, W. A., and Matthews, B. W. (1996) *J. Mol. Biol.* **259,** 542–559
49. Sinha, D., Esumi, N., Jaworski, C., Kozak, C. A., Pierce, E., and Wistow, G. (1998) *Mol. Vis.* **4,** 8
50. Everett, C. A., Glenister, P. H., Taylor, D. M., Lyon, M. F., Kratochvilova-Loester, J., and Favor, J. (1994) *Genomics* **20,** 429–434
51. Favor, J. (1983) *Mutat. Res.* **110,** 367–382
52. Favor, J. (1984) *Genet. Res.* **44,** 183–197
53. Wang, K., Cheng, C., Li, L., Liu, H., Huang, Q., Xia, C. H., Yao, K., Sun, P., Horwitz, J., and Gong, X. (2007) *Invest. Ophthalmol. Vis. Sci.* **48,** 3719–3728
54. Flaugh, S. L., Mills, I. A., and King, J. (2006) *J. Biol. Chem.* **281,** 30782–30793
55. Greene, R. F., Jr., and Pace, C. N. (1974) *J. Biol. Chem.* **249,** 5388–5393
56. Clark, A. C., Sinclair, J. F., and Baldwin, T. O. (1993) *J. Biol. Chem.* **268,** 10773–10779
57. Fu, L., and Liang, J. J. (2003) *Invest. Ophthalmol. Vis. Sci.* **44,** 1155–1159
58. Chen, J., Flaugh, S. L., Callis, P. R., and King, J. (2006) *Biochemistry* **45,** 11552–11563
59. Flaugh, S. L., Kosinski-Collins, M. S., and King, J. (2005) *Protein Sci.* **14,**

2030–2043
60. Kosinski-Collins, M. S., and King, J. (2003) *Protein Sci.* **12,** 480–490
61. Mills-Henry, I. (2007) *Stability, Unfolding, and Aggregation of the Gamma D and Gamma S Human Eye Lens Crystallins*. Ph.D. thesis, Massachusetts Institute of Technology, Cambridge, MA
62. Dobson, C. M. (2004) *Semin. Cell Dev. Biol.* **15,** 3–16
63. Chen, J., Toptygin, D., Brand, L., and King, J. (2008) *Biochemistry* **47,** 10705–10721
64. Mills, I. A., Flaugh, S. L., Kosinski-Collins, M. S., and King, J. A. (2007) *Protein Sci.* **16,** 2427–2444
65. Ishikawa, K., Nakamura, H., Morikawa, K., and Kanaya, S. (1993) *Biochemistry* **32,** 6171–6178
66. Liu, Y., and Eisenberg, D. (2002) *Protein Sci.* **11,** 1285–1299
67. Bax, B., Lapatto, R., Nalini, V., Driessen, H., Lindley, P. F., Mahadevan, D., Blundell, T. L., and Slingsby, C. (1990) *Nature* **347,** 776–780
68. Wahlbom, M., Wang, X., Lindström, V., Carlemalm, E., Jaskolski, M., and Grubb, A. (2007) *J. Biol. Chem.* **282,** 18318–18326
69. Knaus, K. J., Morillas, M., Swietnicki, W., Malone, M., Surewicz, W. K., and Yee, V. C. (2001) *Nat. Struct. Biol.* **8,** 770–774
70. Eakin, C. M., Attenello, F. J., Morgan, C. J., and Miranker, A. D. (2004) *Biochemistry* **43,** 7808–7815
71. Yamasaki, M., Li, W., Johnson, D. J., and Huntington, J. A. (2008) *Nature* **455,** 1255–1258
72. Meehan, S., Berry, Y., Luisi, B., Dobson, C. M., Carver, J. A., and MacPhee, C. E. (2004) *J. Biol. Chem.* **279,** 3413–3419
73. Papanikolopoulou, K., Mills-Henry, I., Thol, S. L., Wang, Y., Gross, A. A., Kirschner, D. A., Decatur, S. M., and King, J. (2008) *Mol. Vis.* **14,** 81–89
74. Marsili, S., Salganik, R. I., Albright, C. D., Freel, C. D., Johnsen, S., Peiffer, R. L., and Costello, M. J. (2004) *Exp. Eye Res.* **79,** 595–612